

Technical University of Denmark



The effect of minor alloying elements in ferritic steels for interconnects in SOFCs

Schuisky, M.; Rosberg, A.; Mikkelsen, Lars; Hendriksen, Peter Vang; Christiansen, N.; Larsen, J. Gutzon

Publication date:
2006

[Link back to DTU Orbit](#)

Citation (APA):

Schuisky, M., Rosberg, A., Mikkelsen, L., Hendriksen, P. V., Christiansen, N., & Larsen, J. G. (2006). The effect of minor alloying elements in ferritic steels for interconnects in SOFCs. Abstract from 2006 Fuel Cell Seminar, Honolulu, HI, United States.

DTU Library

Technical Information Center of Denmark

General rights

Copyright and moral rights for the publications made accessible in the public portal are retained by the authors and/or other copyright owners and it is a condition of accessing publications that users recognise and abide by the legal requirements associated with these rights.

- Users may download and print one copy of any publication from the public portal for the purpose of private study or research.
- You may not further distribute the material or use it for any profit-making activity or commercial gain
- You may freely distribute the URL identifying the publication in the public portal

If you believe that this document breaches copyright please contact us providing details, and we will remove access to the work immediately and investigate your claim.

The Effect of Minor Alloying Elements in Ferritic Steels for Interconnects in SOFCs

M. Schuisky¹, A. Rosberg¹, L. Mikkelsen², P.V. Hendriksen², N. Christiansen³ and J. Gutzon Larsen³

¹AB Sandvik Materials Technology, SE-81181 Sandviken / Sweden

Tel.: +46-26-264083; Fax: +46-26-264177; Mikael.schuisky@sandvik.com

²Fuel Cell & Solid State Chemistry Dept., Risø National Laboratory, DK-4000 Roskilde / Denmark

³Topsoe Fuel Cells A/S, Nymølley 55, DK-2800 Lyngby / Denmark

Abstract

The influence on oxidation resistance as well as conductivity, by the addition of the minor alloying elements Mo and Nb to ferritic chromium steels have been investigated. Especially, effect of trapping silicon inside the alloy matrix by the addition of Mo and Nb has been studied. Three melts with the addition of Mo and Nb and one melt with no Mo and Nb have been studied. The steel melts investigated were produced by a conventional steel making process. The materials were further processed down to cold rolled strips with a thickness of 0.2 mm. The oxidation in air, of coupons of the different model alloys, was studied. The formed oxide scales were further investigated by means of X-ray diffraction, scanning electron microscopy combined with energy dispersive spectroscopy. The area specific electrical interface resistance between the steel alloys and a LSM plate was measured in air at 750°C.

Introduction

In recent years several different ferritic chromium alloys have been suggested as the candidate material for interconnects in solid oxide fuel cells (SOFC) [1,2]. The demand on the life time of interconnect in a SOFC is 40 000 operating hours. The features which makes chromia forming ferritic steels the prime candidate materials for interconnects is, low production costs, good corrosion resistance, ductility and flexibility in comparison to ceramic interconnects and the thermal expansion which is close to the ceramic materials used in SOFC's [3]. Steel producers and other developers have put down a great effort in developing alloys with an expected lifetime of 40 000 hours [1-8]. One of the key elements identified in ferritic steels for the use as interconnect has been silicon. Even though silicon containing steel have successfully been used as interconnect in SOFCs for up to 13 000 hours, silicon is one of the elements which will effect the degradation of the fuel cell [9]. If ferritic chromium steel with a too high silicon content is used this will lead to the formation of silicon oxide under the formed chromium oxide scale. [10-11] The formation of electrically insulating silicon oxide will increase the electrical resistance of the surface and by doing so decrease the over all efficiency of the fuel cell. This have lead to the production of low silicon containing alloys by either using very pure starting material or by vacuum melting processes, both which will add cost to the production of the material. However, by carefully alloying the ferritic steel with the right elements the small amount of silicon normally occurring in conventional produced steel can be trapped in the steel matrix in the form of silicon containing particles. The entrapment of silicon inside the alloy matrix, will reduced the risk of formation of silicon oxide under the chromia scale. Chromium poisoning is another source that causes degradation of the fuel cell which is believed to be solve by protective coatings of interconnects of ferritic chromium steel.

Experimental

In this studied four model alloys of ferritic chromium steel with 22% chromium were produced by ordinary steel manufacturing processes. Especially, effect of trapping silicon inside the alloy matrix by the addition of Mo and Nb has been studied. Three melts with the addition of Mo and Nb and one melt with no Mo and Nb were produced. The materials were further processed to cold rolled strips with a final strip thickness of 0.2 mm. The chemical compositions of the alloying elements of the materials referred to in this study are listed in table 1 below, together with the designated

names of the model alloys. The samples were cooled to room temperature before measuring the weight gains at 168 hours intervals. The samples were oxidized for a total of 1008 hours. For phase identification studies of the formed oxide scales, x-ray diffraction (XRD) was performed using a Bruker D8 Discover diffractometer. The surface morphologies as well as the cross sectional micrographs of the oxide scales were investigated utilizing a Leo DSM 962 scanning electron microscope (SEM) equipped with Energy Dispersive Spectroscopy (EDS) for elemental analysis. The electrical interface resistances between LSM plates and the alloys were measured by a DC four-point method in air at 750°C over a period of 1000 h. A contact layer of (La,Sr)(Mn,Co)O₃ was applied between the alloys and LSM plates. Experimental details are given in [12].

Table 1. The amount of alloying elements added to 22% ferritic chromium steels investigated.

Name	Si	Mn	Mo	Nb	Ti + Zr	Other add.
#520	0,2	0,3	1,0	0,9	0,3	
#522	0,2	0,4	1,0	0,4	0,3	
#524	0,4	0,4	0,6	0,4	0,3	
#527	0,2	0,4	0	0	0,03	Ce = 0.03

Results and discussion

An oxidation study was done on coupons of all four alloys at 850°C in air for 1008 hours. The weight gains of two coupons of each alloy were measured with intervals of 168 hours and the area specific weight is plotted versus time in Fig. 1. In the figure below it can clearly be seen that the 3 alloys i.e. #520, #522 and #524 with the addition of Mo, Nb and Ti/Zr shows the best oxidation resistance compared to the almost pure 22% Cr alloy i.e. #527 with a small addition of Ce. The model alloys with a Mo and Nb addition all had very similar oxidation behaviour despite the different amounts of Mo and Nb added. They all ended up with a weight gain of about 0.7 mg/cm² after 1008 hours of oxidation at 850°C in air. It appears that a small addition of a rare earth metals such as Ce to a ferritic chromium steel will not have as positive effect on the corrosion resistance as the addition of Mo, Nb and group IV metals. The #527 model alloy with no Mo and Nb added had the worst corrosion resistance with a weight gain of 1,8 mg/cm² after 1000 hours oxidation at 850°C in air.

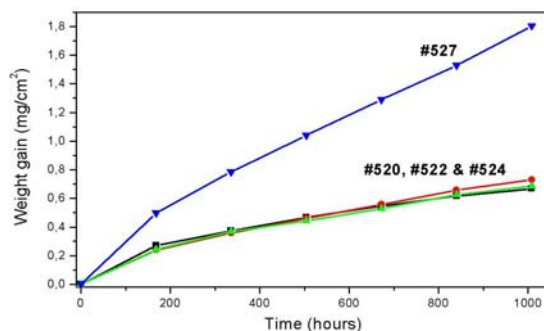


Fig. 1. Weight gain of the four different model alloys as a function of time while oxidized in air at 850°C.

The cross section of the oxidized samples scales were investigated by SEM/EDS. The alloying elements were mapped by EDS and below is the EDS mapping of the oxide scale formed on the model alloy #527. In Fig. 2 a rather thick oxide scale of about 15 μm was observed consisting of a Mn rich outer part followed by a Cr richer oxide and thin but appearing silicon oxide layer below the chromia scale. However, in the Mo and Nb alloyed steel with the same amount of Si i.e. 0.2% by weight no formation of a silicon oxide layer under the chromia scale was observed. Instead the silicon was entrapped in Mo-Nb-Si rich particles inside the steel matrix.

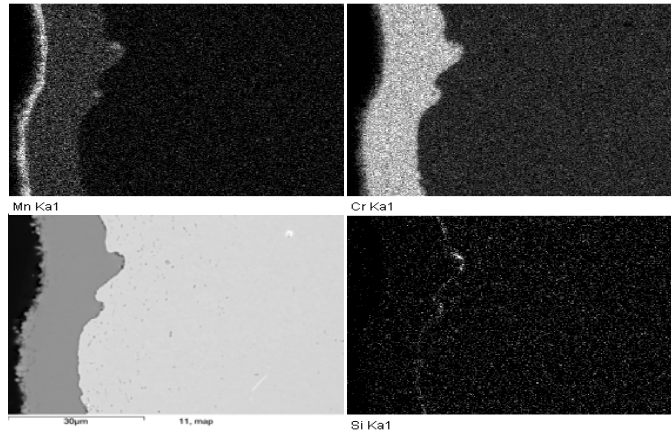


Fig. 2. SEM/EDS mapping of alloying elements Mn, Cr and Si in the model alloy #527.

This is very well illustrated in Fig. 3 below which shows a SEM/EDS cross section of the formed oxide scale on the model alloy #522. In the EDS element mapping of Si, Nb and Mo it is seen that the 3 elements are forming well dispersed particles inside the alloy matrix. Furthermore it can be seen that both model alloys forms duplex oxide scales which have been formed after 1008 hours of oxidation in air at 850°C. The outer part of the scale contains a more Mn rich oxide, confirmed by X-ray diffraction to have a spinell structure, followed by a more chromium rich oxide and under this a Ti enriched thin oxide layer. However, more important and interesting is that despite the fact that this particular alloy contained more than 0.2% silicon almost no string of silicon is detected under the oxide scale. Instead the silicon is detected in particles inside the steel matrix. In the mapping it is very easy to see that the elements bonded to the silicon are Mo and Nb. Similar behaviour have just recently been observed for W & Nb alloyed ferritic steels. [X]

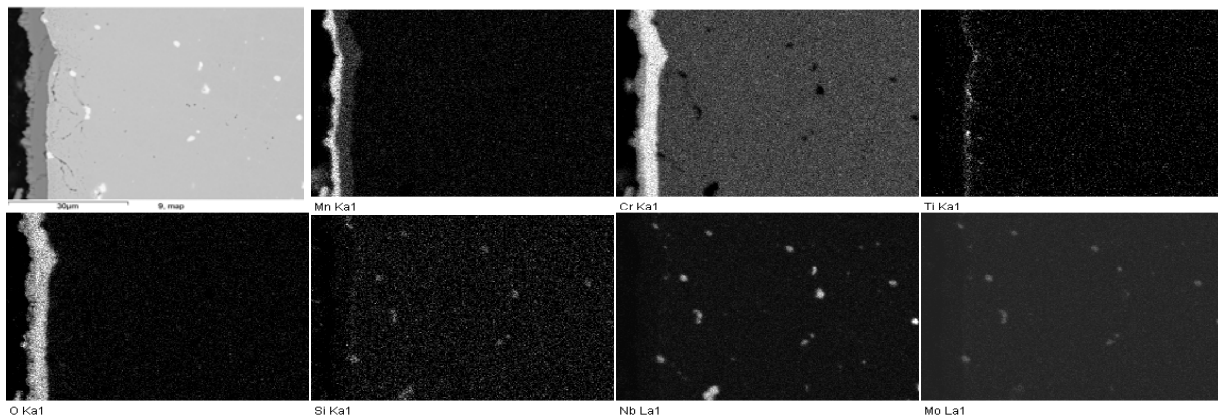


Fig. 3. SEM/EDS mapping of alloying elements in the Mo-Nb-Si alloyed melts #522.

More important than only oxidation resistance is the area specific resistance (ASR) values of the model alloys and the alloy-LSM plate interfaces were measured during aging at 750°C. The ASR-values for the alloys are shown in Fig. 4. The largest degradation rate was found for the #527 alloy with a degradation of more than $7 \text{ m}\Omega\text{cm}^2/10^3 \text{ h}$. The much thicker oxide scale and the appearance of silicon oxide under the chromia scale of the #527 alloy is likely the cause of this degradation rate. The 3 model alloys with the addition of Mo and Nb all had a higher degradation rate during the first 200 hours. Especially, the ASR curve for the model alloy #524 made a large initial increment of the ASR during the first 100 hours but then it dropped and decreased the ASR back till almost the same as the initial value. A possible reason for the increment of the ASR initially is the formation of a more pure chromia scale which by time is converted to a more duplex Mn spinell containing surface oxide due to diffusion of Mn out to the surface from the bulk of the alloy. The 3 Mo and Nb alloyed model alloys all are showing both good corrosion protection properties as well

as good electrical performance at high temperature and is therefore a good candidate material for interconnects in SOFCs.

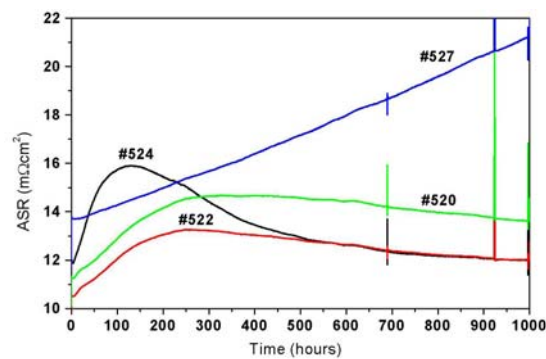


Fig. 4. Electrical interface resistance between the four model alloys and LSM plates measured during aging at 750°C, include a contribution from a LSM plate (~ 7 mΩcm²).

Conclusion

It has here been observed that by alloying ferritic chromium steel with Mo and Nb the remaining silicon in the alloy can be entrapped by the formation of Mo-Nb-Si particles. The formation of silicon rich particles inside the alloy matrix will lower the risk of formation of silicon oxide under the chromia scale. This will lead to lowering the electrical resistance cause by the oxidation of the steel interconnect. These newly developed alloys are much better candidate materials than the 22% Cr alloy with a small amount Ce used as reference.

Furthermore, this will lead to much simpler production routes of the stainless steel for interconnects since no advanced vacuum melting processes are needed or no need for high purity starting material is needed.

References

1. W.J. Quadackers, J. Piron-Abellan, V. Shemet and L. Singheiser, *Mat. High Temp.* **20**, 115-127, 2003.
2. Z. Yang, K. S. Weil, D. M. Paxton and J. W. Stevenson, *J. Electrochem. Soc.*, **150** 1188-1201, 2003.
3. S. Linderoth and P.H. Larsen, *Mater. Res. Soc. Symp. Proc.*, **575**, 325-330, 2000.
4. T. Uehara, T. Ohno and A. Toji, *Proc. of the 5th European SOFC Forum*, **1**, 281-288, 2002.
5. J. Pirón-Abellán, F. Tietz, V. Shemet, A. Gil, T. Ladwein, L. Singheiser and W. J. Quadackers, *Proc. of the 5th European SOFC Forum*, **1**, 248-256, 2002.
6. T. F. Pedersen, S. Linderoth and J. Laatsch, *Proc. of the 6th European SOFC Forum*, **2**, 897-907, 2004.
7. A. R. Dinesen, K. A. Nielsen, F. W. Poulsen, L. Mikkelsen and P. V. Hendriksen, *Proc. of the 6th European SOFC Forum*, **2**, 940-950, 2004.
8. L. Mikkelsen, P.H. Larsen and S. Linderoth, *J. Therm. Anal. Cal.*, **64**, 879-886, 2001.
9. N. Christiansen, S. Kristensen, H.H. Larsen, P.H. Larsen, M. Mogensen, P.V. Hendriksen, *Proc. of the Electrochem. Soc. SOFC IX, Vol. 2005-07*, 2005.
10. A. N. Hansson, Ph.D. report, IPL, Technical University of Denmark, 2004.
11. M. Schuisky, A. Rosberg, L. Mikkelsen, S. Linderoth, N. Christiansen and J. Gutzon-Larsen, *Proc. of the 26th Risø Int. Symp. Mater. Sci.*, 329-334, 2005.
12. L. Mikkelsen, A. R. Dinesen and P. V. Hendriksen, *Proc. of the Electrochem. Soc. SOFC IX, Vol. 2005-07*, 1832-1841, 2005.
13. L. Mikkelsen, S. Linderoth and J. B. Bilde-Sørensen, *Mater. Sci. Forum* **461-464**, 117-122, 2004.
14. P. Huczowski, N. Christiansen, V. Shemet, J. Prion-Abellan, L. Singheiser and W. J. Quadackers, *Mater. Corr.*, **55**, 825-830, 2004.